NEUTRONIC AND SAFETY ASPECTS OF A GAS-COOLED SUBCRITICAL CORE FOR MINOR ACTINIDE TRANSMUTATION

THERMAL HYDRAULICS

KEYWORDS: *accelerator-driven systems, helium cooling, minor actinide fuel*

DANIEL WESTLÉN* and JANNE WALLENIUS
Royal Institute of Technology, Department of Nuclear and Reactor Physics
S-106 91 Stockholm, Sweden

Received June 18, 2004
Accepted for Publication July 20, 2005

We have designed a gas-cooled accelerator-driven system dedicated to transmutation of minor actinides. Thanks to the excellent neutron economy of the uranium-free fuel employed, the pin pitch to diameter ratio (P/D) could be increased to 1.8. The increased coolant fraction allows for decay heat removal at ambient pressure. The large coolant fraction further results in a low pressure loss—26 kPa over the core, 35 kPa in total. Thanks to the large P/D, the elevation of the heat exchanger necessary to remove decay heat by natural circulation is just more than 1 m. The absence of uranium in conjunction with the presence of 35% (heavy atom) americium in the fuel results in a low effective delayed neutron fraction and a vanishing Doppler feedback, making subcritical operation mandatory.

I. INTRODUCTION

Transuranium elements in spent light water reactor (LWR) fuel remain radiotoxic at a level above that of uranium in nature for more than 100 000 yr. By separation and subsequent transmutation of these elements, the required time for storing the residual waste may be reduced to >1000 yr (Refs. 1 and 2). Plutonium may be multirecycled in fast reactors or in existing LWRs using mixed-oxide (MOX) fuel with the support of enriched uranium.[3] However, if one does not transmute americium and curium, the reduction in radiotoxic inventory becomes marginal. Recycling of americium and curium in LWRs, however, leads to an increase of neutron emission rates during reprocessing by three orders of magnitude.[2] Therefore, higher actinides should be recycled in a fast neutron spectrum.

*E-mail: daniel@neutron.kth.se

Introducing americium into the fuel of fast critical reactors leads to safety concerns; since the Doppler feedback is reduced, the effective delayed neutron fraction decreases and the coolant void coefficient becomes more positive.[4] These three effects in combination limit the potential for transmuting americium in fast reactors. Transmutation of americium-rich fuels might be accomplished, however, by the implementation of fast neutron accelerator-driven systems (ADSs), as first suggested by Foster et al.[5] Several designs of such systems have been proposed.[6–8]

The main difference between a critical reactor and an ADS is that a spallation source driven by a proton accelerator is used to supply source neutrons. Spallation targets for high-power ADSs are typically suggested to consist of liquid lead-bismuth alloy. The design of the core itself is more of an open issue being subject to intense research efforts. Candidates for fuel composition are oxides, nitrides, and metals.

Lead-bismuth eutectic (LBE) or sodium have been considered as coolants.[6,7] The main reason to use a liquid metal as a coolant is because of the high thermal conductivity found in most metals. Among drawbacks pertaining to liquid-metal coolants are the incompatibility with water of sodium and the corrosion problems associated with lead and lead alloys.

Gas cooling is therefore an interesting alternative to the liquid-metal coolants. Among the possible gases, helium features the most suitable characteristics.[9] Helium provides a hard neutron spectrum, which is beneficial for limiting buildup of curium and other heavier elements. A low chemical reactivity of the coolant—as in the case of helium—is a prerequisite if high temperature operation is to be feasible. Further, the optical transparency allows for visual inspection of the core, which is not possible in metal-cooled systems.

However, the main disadvantage of using helium coolant is the low density, which implies that high pressure operation is necessary to ensure heat removal. Typically fast helium-cooled reactors are designed to operate at

pressures between 8 and 12 MPa (Ref. 9). A loss-of-pressure or loss-of-flow accident might consequently lead to severe difficulties in removing decay heat. Several approaches have been suggested to address this issue.[10,11]

We suggest utilizing the excellent neutron economy of uranium-free plutonium-based fuels to increase the coolant mass flow through the core by increasing the pin pitch to diameter ratio (P/D). An increased P/D may relieve issues related to loss-of-pressure and loss-of-flow accident scenarios.

In what follows we will account for a design of a gas-cooled ADS that guarantees decay heat removal at ambient pressure or under natural circulation conditions. We start by showing how the introduction of americium into the fuel of gas-cooled reactors reduces Doppler feedback and effective delayed neutron fractions. We then present the fuel composition and core geometry assumed in this study. We continue by showing how the core proposed is expected to behave during a severe loss-of-pressure accident and during a loss-of-flow accident. Finally, we conclude by giving some preliminary results concerning neutronic properties of the system, evaluating the transmutation capability of the proposed design.

II. IMPACT OF AMERICIUM ON SAFETY PARAMETERS

The safety of critical fast reactors relies on negative feedbacks that compensate for potential reactivity insertions. The negative feedback from radial expansion of the core diagrid typically is larger than the positive feedback from coolant expansion and manages to stabilize the core in the case of slow transients like loss of flow and loss of heat sink. For rapid excursions, which in fast reactors always may occur as a result of core compaction, it is important that prompt negative feedbacks like Doppler broadening and/or axial expansion of the fuel have a significant magnitude. Further, the effective delayed neutron fraction may not be too small.

When introducing americium into the fuel of fast reactors, the magnitude of the Doppler feedback and beta effective is reduced. This is because americium has a much higher cross section for capture than ^{238}U, ^{240}Pu, or ^{232}Th. Thus, neutrons under moderation are captured by americium in the unresolved resonance range, where Doppler broadening is much more inefficient than for captures in resolved resonances at lower energies. Similarly, the large cross section for capture in americium means that delayed neutrons, being born with an average energy of 0.5 MeV, have a smaller probability of inducing fission than in an americium-free fuel. Figure 1 displays the capture cross section of ^{241}Am and ^{238}U. Even though there is an uncertainty in the evaluated data sets, it is clear that even a relatively small fraction of Am in the fuel will have a significant impact on the capture rate in different nuclides.

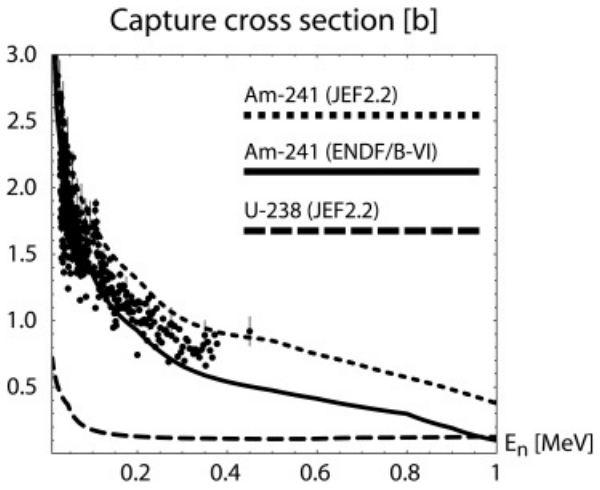

Fig. 1. Evaluated (JEFF3.0) capture cross section of ^{241}Am and ^{238}U.

In order to quantify this impact, we have calculated beta effective and the Doppler constant for a simplified pin cell model of the gas-cooled fast reactor (GCFR) design developed in the United States during the 1960s (Ref. 12). The model consists of a radially infinite pin lattice with P/D = 1.45. The calculation was made with the Monte Carlo code MCB1C, using the JEFF3.0 cross-section library Doppler broadened at temperatures of 1200 and 1800 K, including probability tables for absorption in the unresolved resonance region. Table I compares the Doppler constant $K_D = T\ dk/dT$ and β_{eff} of the reference oxide fuel with fuels where part or all of the uranium has been substituted with americium or zirconium. As expected, the Doppler constant of the reference fuel is smaller than for liquid-metal–cooled fast breeder reactors but corresponds to a feedback comparable to that of axial

TABLE I

Change in Doppler Effect and β_{eff} with Increasing Fuel Am Content*

U	Pu	Am	Zr	$K_D = T\ dk/dT$	β_{eff}
80	20	—	—	−285 (11)	503 (25)
70	20	10	—	−88 (11)	473 (23)
50	20	30	—	0 (14)	356 (32)
—	20	30	50	+10 (16)	227 (38)
Reference value[13]				−320	—
Calculated reference value				−388 (13)	—

*The Doppler effect is significantly weakened and the value of β_{eff} diminishes when Am is introduced in the fuel. Values in parentheses indicate one standard deviation. The geometry of the reference core is assumed for all cases.

expansion of ceramic fuels, i.e., −0.2 pcm/K. The value obtained in our simplified model is on good agreement with full core calculations for the GCFR design.[13] When introducing americium into the fuel, one sees that the Doppler constant is dramatically reduced, even in the presence of ^{238}U. This is well in line with calculations previously made by one of the present authors for sodium-cooled systems.[14] Thus, for fast neutron cores dedicated to transmutation of the higher actinides, it will only be possible to regain a significant Doppler feedback if the ratio of Am to ^{238}U in the fuel is less than ~1 to 7. The effective delayed neutron fraction also decreases. The reduction is not as large as for the Doppler, but it does mean that any reactivity insertion has a considerably higher worth than in the case of an americium-free fuel.

One may thus conclude that burning of the minor actinide waste of present LWR parks in fast spectra requires a relatively large dilution of americium in uranium and therefore a large fraction of fast neutron reactors in the system operating on advanced fuels. Therefore, it is of interest to investigate the option of minor actinide burning in subcritical reactors, which may be loaded with a much higher fraction of americium.

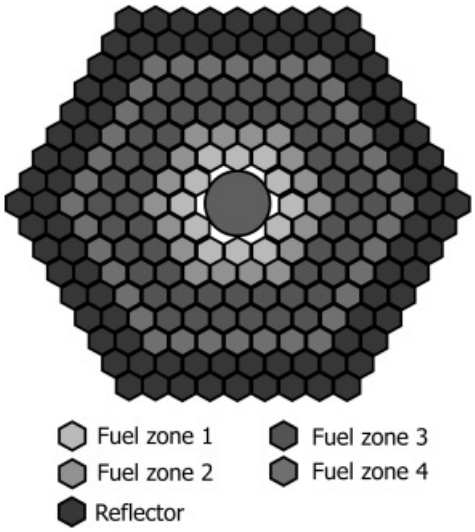

Fig. 2. Core map for the present design. Fuel zones distinguished by different shades of gray correspond to plutonium concentrations of 28, 34, 45, and 100%, respectively.

III. GAS-COOLED ADS CORE AND FUEL DESIGN

In conventional fast reactor designs, achieving a high breeding ratio has been the primary concern. Consequently, the reduction of neutron leakage has been an important design parameter. In contrast, uranium-free fuels dedicated to waste transmutation feature a neutron surplus that may be used to improve transmutation performance and core safety.

We have based our ADS design on the GCFR (Ref. 12). Seven of the central fuel assemblies are removed to make place for the spallation target. As in the GCFR, four fuel zones with different ratios between fertile and fissile nuclides are used to minimize the radial power peaking factor. At beginning of life (BOL), the reflector is loaded with boron carbide assemblies that batchwise are replaced with steel pin assemblies in order to manage reactivity losses. The corresponding core map is shown in Fig. 2. The active height of the core was decreased from 1.15 to 1.0 m to minimize the axial power peaking factor. This leads to increased axial neutron leakage, which, however, may be afforded because of a better neutron economy. We have adopted fuel clad dimensions identical to that of the GCFR, that is, an inner/outer diameter of 7.1/7.8 mm. The P/D has been increased as much as possible in order to maximize the coolant flow area. Thus, the working pressure as well as the pressure loss over the core are reduced, mitigating consequences of loss-of-pressure and loss-of-pumping–power accidents.

In line with recent studies of GCFRs in France,[15] we have selected nitride fuel for the present design because of its high power to melt and the relative ease of reprocessing. A fuel porosity of 15% was adopted to allow for solid fission product swelling. Nitrogen enriched in ^{15}N is assumed to be used in order to avoid the production of ^{14}C. A ^{15}N content of 98% has been shown to be sufficient for the ^{14}C production in minor actinide–burning ADS cores to be less than the production of ^{14}C in the oxide fuel of LWRs (Refs. 16 and 17). The main disadvantage of nitride fuels, however, is the high vapor pressure of americium, which requires the use of a stabilizing inert matrix like zirconium nitride.[18] Recent tests of (Pu,Zr)N fabrication by nitridation of metals at relatively low temperature have shown that a solid solution is only obtained for matrix volume fractions above 60 at.% (Ref. 19). We therefore fix the ZrN fraction in the fuel to 60% in the entire core and adjust the ratio between plutonium and higher actinides in the fuel to obtain a k eigenvalue of 0.97 at BOL. Further, the Pu/minor actinide ratio is differentiated over the fuel zone in order to achieve a radial power peaking factor <1.2. Increasing P/D, the relative fraction of plutonium must thus be raised.

Neutronics calculations were performed using the Monte Carlo continuous energy burnup code MCB (Refs. 20 and 21), which is based on MCNP4C and allows for a complete treatment of fuel burnup. All core design calculations were performed using a fully three-dimensional pin by pin model, including axial and radial reflectors. Assuming an actinide vector corresponding to that of spent LWR MOX fuel (see Table II), we find that the plutonium content in the outermost fuel zone becomes 100% for P/D ≈ 1.8.

The core geometry parameters are summarized in Table III. As we have a larger P/D, the number of fuel

TABLE II

Isotopic Compositions of Actinides in the Fuel

^{238}Pu	5.1%	^{241}Am	66.6%
^{239}Pu	37.9%	^{243}Am	33.4%
^{240}Pu	30.3%		
^{241}Pu	13.2%	^{244}Cm	87.3%
^{242}Pu	13.5%	^{245}Cm	12.7%

TABLE III

Core Geometry Parameters

Property	Present Design
Core height (m)	1.00
Fuel pin inner/outer diameter (mm)	7.1/7.8
Fuel-clad gap (mm)	0.05
Pellet diameter (mm)	7.0
P/D	1.7806
Assembly wall thickness (mm)	4.0
Assembly spacing (mm)	2.0
Assembly inner flat to flat (FTF) (mm)	178.4
Assembly outer FTF (mm)	185.3
Number of fuel assemblies	120
Number of rods	20 280

pins per subassembly (169) as well as in the entire core (20 280) is lower than for the GCFR design. We have chosen not to increase the linear rating of the fuel in order to keep down the working pressure. Hence, the total core power will be reduced.

Figure 3 is an example of the shape of the power distribution at BOL for plutonium concentrations of 28/34/45/100% actinide atoms in the four fuel zones. These fractions correspond to a core-averaged composition of 58% Pu, 35% Am, and 7% Cm. Considering that spent LWR MOX fuel contains Pu and higher actinides in a proportion of 4 to 1 (Ref. 22), 30% of the Pu produced in LWRs could be incinerated in the present ADS, the remaining 70% being multirecycled in LWRs.

The contribution of neptunium to the radiotoxic inventory of spent LWR fuel is less than the radiotoxicity in natural uranium[22] (ingestion dose 20 mSv/g) and is hence not significant. For this reason, we chose not to include neptunium in our transmutation strategy.

IV. THERMAL-HYDRAULIC ANALYSIS

Having fixed P/D to 1.8 from neutronic considerations, we should settle on a linear rating and a total core power. While a low rating is beneficial from the safety viewpoint, economy drives toward higher power densities. We have chosen to require that decay heat should be possible to remove at ambient pressure (one atmosphere) for a coolant velocity of 70 m/s. The coolant temperature in an arbitrary axial position z_1 is given by the sum of the inlet temperature and the integral of the heat flux, $q(z)$, from the pin to the coolant:

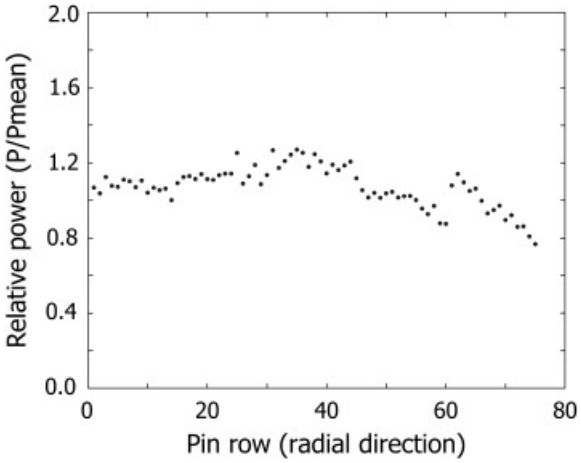

Fig. 3. Example of radial power profile in the core. Each dot corresponds to the calculated power in a single rod. The estimated error of the Monte Carlo calculation is 3%.

$$T_{cool} = T_0 + \int_0^{z_1} \frac{q(z)}{\dot{m} \cdot c_p} dz \ . \quad (1)$$

The cladding temperature is given by the relation

$$q(z) = h[T_{clad}(z) - T_{cool}(z)] = \frac{\chi(z)}{2\pi R_{clad}} \ , \quad (2)$$

where $\chi(z)$ is the linear power. The heat transfer coefficient h is expressed as

$$h = \frac{k}{D_h} \cdot \mathrm{Nu} \cdot SR \cdot C \ , \quad (3)$$

where D_h is the hydraulic diameter. The thermal conductivity k varies by about a factor of 3 for helium over the temperatures of interest. The geometry of the ribs on the cylindrical rods is chosen so that the surface roughening factor *SR* equals 2 (Refs. 9 and 23). *C* is a boundary layer correction factor, which we chose to put to unity.[23] In our case, the main contribution to the Nusselt number Nu is convection. We have adopted the Dittus-Boelter correlation for the Nusselt number:

$$\mathrm{Nu} = 0.023 \mathrm{Re}^{0.8} \mathrm{Pr}^{0.4} \ . \quad (4)$$

Thermophysical data for helium as a function of temperature and density were taken from the literature.[24,25]

For P/D = 1.8, a pressure of one atmosphere, a velocity of 70 m/s, and a decay heat power of 1.4 kW, we allow a maximum cladding temperature of 1300 K, the inlet temperature adjusted to meet this condition. Transient tests of D9 cladding tubes irradiated up to 100 displacements per atom (dpa) have been performed at heating rates of 110 K/s, showing that a hoop stress of 120 MPa leads to clad burst at 1300 K (Ref. 26). Such a hoop stress corresponds to a differential pressure of 11 MPa at 1300 K. As will be shown later, the internal gas pressure in the hottest fuel pin will not exceed 6.0 MPa under normal operation. Hence, it is likely that D9, or similar steels like the 15-15Ti clad developed for use in Phenix, would survive the here postulated loss-of-pressure accident at the given decay heating rate. Eventually, the grace time to failure would depend on thermal creep rates. Data on D9 indicate that the clad may survive up to 10 min at 1300 K and up to 1 h at 1200 K (Ref. 27). Since the decay heating rate decreases by more than a factor of 2 within a few minutes, it appears the clad would remain intact.

Having fixed the operating pressure, P/D, and the upper cladding temperature during a potential accident, the average linear power of the hottest fuel pin is given by the assumption that the decay heat corresponds to 5% of full power. We have chosen to limit it to 28 kW/m (axial average), considerably lower than that of the GCFR design. Our postulated loss-of-pressure scenario thus appears to be more restrictive than that assumed for GCFR.

We may now calculate the core working pressure. As will be shown later, the full release of all fission gases and helium generated in the fuel leads to an internal gas pressure of <6.0 MPa at end of life (EOL). The corresponding hoop stress is 64 MPa, which is just below one-third of the tensile yield strength for 15-15Ti cladding tubes at a temperature of 1000 K (Ref. 28). Abiding thus to the Règles d'Analyse Mècaniques des Stuctures criterion of the Commissariat à l'Energie Atomique[29] indicates that 1000 K should be taken as the temperature limit for our clad under normal operation. We chose, however, to stay conservative and have adopted 900 K as the limit. As shown in Fig. 4, the hot spot temperature in the core remains below 900 K for a coolant pressure exceeding 4.3 MPa. As the maximum linear power of our design, 28 kW/m, is lower than for the GCFR reference design, the inlet temperature may be somewhat higher without exceeding the temperature limits for core damage. The inlet temperature is 577 K as compared to 560 K for the GCFR. We summarize the thermal characteristics of the core in Table IV.

Concerning the core performance under a loss-of-pumping–power event, one needs to show that natural circulation can achieve decay heat removal. We have assumed turbulent flows as Reynolds numbers exceed 2500, the Reynolds number given from

$$\mathrm{Re} = \frac{\rho U D_h}{\mu} \quad . \tag{5}$$

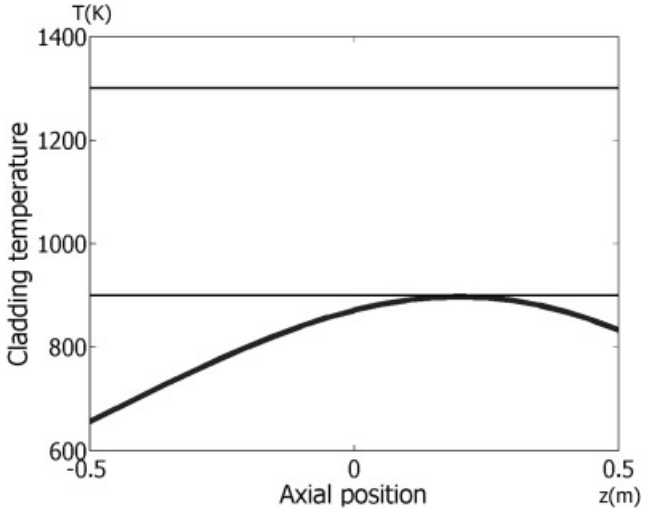

Fig. 4. Under normal operation at 4.3 MPa and a coolant velocity of 70 m/s, the hot spot temperature never exceeds 900 K.

TABLE IV

Core Thermal-Hydraulics Characteristics

Total core power [MW(thermal)]	570
Average linear power (kW/m)	28
Operating pressure (Pa)	4.3×10^6
Coolant flow speed (m/s)	70
Max cladding temperature—operation[29] (K)	900
Max cladding temperature—accident[37] (K)	1330
Coolant inlet temperature (K)	577
Surface roughening factor[23]	2

The coolant density, velocity, and viscosity are denoted by ρ, U, and μ, respectively.

The frictional pressure drop over the core is given by[30]

$$\Delta p_f = 2(f_r L_r + f_s L_s)\,\frac{1}{D_h}\cdot\frac{G^2}{\rho} \quad , \tag{6}$$

where $L_r = 1.0$ m and $L_s = 1.5$ m are the heights of the roughened and smooth parts of the coolant channel, respectively. $G = \rho U$ is the mass flux. The rough channel friction factor is given by Melese-d'Hospital as $f_r = 0.05 \cdot \mathrm{Re}^{-0.1}$ (Ref. 30). According to Todreas and Kazimi, the Darcy smooth channel factor friction factor f satisfies $f \cdot \mathrm{Re}^{0.18} = 0.17$ for P/D = 1.8 and turbulent flow.[31] The average density of the helium coolant in our design is 3.5 kg/m^3 at normal operation. With a mass flux of $G = 243$ kg·m^{-2}·s^{-1}, this gives a pressure drop over the coolant channel of 2.6×10^4 Pa. This pressure drop is low compared to other gas-cooled designs, e.g.,

the GA-GCFR design, where the pressure drop over the core was 1.83×10^5 Pa (Ref. 32). The main difference is that our core operates at a lower pressure and that the large P/D in our design reduces coolant channel friction significantly.

We are not concerned that the fuel pin spacers will produce hot spots on the cladding. Hassan and Rehme[33] showed that for high Reynolds numbers, the heat transfer properties are not affected much by the spacers. The effect that actually is seen is a somewhat increased heat transfer around the spacers due to an increase in flow velocity. In any case, we assume the spacers to be located away from the hottest part of the fuel pins.

The flow velocity at natural circulation (denoted by primed variables) is given by[30]

$$U' = \frac{Q'}{c_p A (T'_{out} - T'_{in}) \rho'} \quad . \tag{7}$$

The inlet and outlet temperatures are denoted by T_{in} and T_{out}, respectively. For a standard pin in a triangular lattice, the channel area A is expressed by

$$A = 2 \cdot \left(\frac{\sqrt{3}}{4} \left(\frac{P}{D} \right)^2 - \frac{\pi}{8} \right) D^2 \quad . \tag{8}$$

Natural circulation is governed by the difference in coolant density arising from temperature differences and from the vertical distance ΔL between the thermal centers of the heat exchanger and core, according to

$$\Delta p = g \Delta L (\rho'_{in} - \rho'_{out}) = g \Delta L M_A \frac{p}{R} \frac{\Delta T'}{T'_{in} \cdot T'_{out}} \Rightarrow$$

$$\Delta L_t = \frac{\Delta p R}{g M_A p} \cdot \frac{T'_{in} \cdot T'_{out}}{\Delta T'} \quad . \tag{9}$$

The difference between inlet and outlet temperatures is denoted by ΔT, where Z is a factor relating the pressure drop in the entire system to the pressure drop over the core. Following the GCFR design we have assumed $Z = 4/3$ (Ref. 30).

At the large P/D we propose the pressure drop at low coolant velocities is small. If we assume a loss-of-flow situation without the pressure being lost, the ΔL required is slightly above 1 m. Figure 5 shows how ΔL varies with P/D.

The GCFR design uses 1000 K as the upper cladding temperature during normal operation. We believe this might be somewhat optimistic and have thus assumed 900 K. To achieve a lower top cladding temperature, a lower inlet temperature is necessary. A lower inlet temperature is beneficial for the natural circulation conditions as more heat is removed by the same mass flow when the temperature difference over the core increases. ΔL for the GCFR was 10.4 m (Ref. 30). Our design would require a ΔL of 2.5 m once the 1000 K temperature limit, and the GCFR assumption of a decay heat corresponding to 6% of full power, were to be applied. For smaller P/D we calculate values corresponding to the values given by the reference.[30]

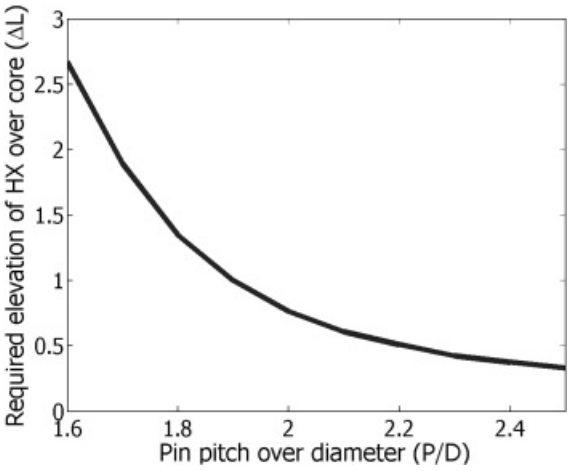

Fig. 5. The elevation of the heat exchanger over the core required for heat removal by natural circulation decreases considerably as P/D is increased.

The pumping power W_p required at normal operation is given by

$$W_P = \Delta p_{tot} \cdot A \cdot U \quad . \tag{10}$$

For the present design, $W_p = 5.9$ MW, which roughly corresponds to 3% of the electrical output from the system.

V. NEUTRONIC SAFETY PARAMETERS

As mentioned previously, both the effective delayed neutron fraction and the Doppler feedback are reduced when americium is introduced in any significant amount. β_{eff} was calculated for the present core using MCNP in two consecutive runs, one with and one without delayed neutrons. The effective delayed neutron fraction was found to be 140 ($\pm$20) pcm. As expected from the pin cell calculations, the Doppler feedback is completely insignificant for the present fuel. Even when comparing k eigenvalues at fuel temperatures of 300 and 1800 K, the calculated difference is merely -0.02 ($\pm$0.01) pcm/K. In a similar vein, the coolant void worth was calculated in two subsequent runs, the first one with He density corresponding to the core average temperature and pressure and the second with a He density relevant for ambient pressure. The k eigenvalue increases by 870 ($\pm$40) pcm at a pressure drop accident. The combination of a 6 \$ positive void worth, zero Doppler, and the low β_{eff} should make subcritical operation of this system mandatory.

VI. BURNUP

Transmutation efficiency is governed by the burnup during irradiation and the losses during reprocessing and fuel fabrication. High burnup reduces the number of reprocessing cycles required, thereby reducing actinide losses, costs, and the time needed to transmute the waste. In a spallation source–driven subcritical core, the reactivity loss due to burnup of the fuel is compensated for by increasing the power of the accelerator beam. Initially, the beam current is ~24 mA. We allow the current to double, but further increase is prohibited because of safety reasons.[14] This means the k eigenvalue drops from 0.97 to 0.94 before we take any action to increase the reactivity. Allowing for large variations in beam power and consequently in neutron source strength could result in erroneously large power insertions leading to fuel damage. In order to compensate for reactivity loss, boron carbide absorber assemblies in the reflector are replaced with steel pin assemblies as burnup proceeds. Consequently, the radial power profile changes with burnup. While the power decreases in the core center, it increases in the periphery.

The factor ultimately limiting burnup in fast neutron systems is irradiation-induced swelling of the fuel cladding. Titanium stabilized cladding steels like 15-15Ti have shown acceptable swelling rates up to irradiation doses of 150 dpa, the expectation being that 180 dpa will be possible with minor optimization.[34] The peak radiation dose rate anywhere in the present core is 44 dpa/yr. Hence, there is a potential for operation under 1500 effective power days. We are able to increase reactivity of our core four times by substituting absorbers in the reflector with steel, each time raising the k eigenvalue from 0.94 back to 0.97. This gives five burnup periods totaling 1400 days and a maximum dose of 170 dpa. The core-averaged actinide burnup is 19.1% at EOL.

The actinide inventory at BOL and EOL is shown in Table V. The decay of ^{238}Pu ($t_{1/2}$ = 87.7 yr) and ^{244}Cm ($t_{1/2}$ = 18.1 yr) out of pile gives rise to (α, n) reactions. Their concentrations at EOL are therefore likely to be the main cost drivers for fuel reprocessing and manufacturing. Curium-242 with a half-life of 162.8 days is the main source of helium production in the fuel, causing either fuel swelling or pin pressurization. A core design that minimizes the production of these three nuclides is hence favorable. Figures 6, 7, and 8 show how the buildup of these isotopes varies as a function of core position. Thanks to the hard spectrum achievable with helium cooling, the buildup of curium is insignificant, indicating that the Am/Cm ratio in the start-up fuel composition is similar to that in the equilibrium state. The softening of the spectrum in the outer fuel zone as boron carbide absorber elements in the reflector are removed leads to an increased production rate of curium when approaching EOL. Considering the very small initial concentration of Am and Cm in zone 4, the overall contribution to curium production in zone 4 is insignificant. Still, this is a good illustration of the benefits of a hard spectrum for transmutation of americium. During 1400 days of operation, 0.27 g of helium are produced per rod in fuel zone 1 closest to the spallation target. In zone 4 only 0.01 g are produced per rod.

One-group fission and capture cross sections for the nuclides of major interest are displayed in Tables VI and VII. The removal of the boron carbide absorber in the reflector leads to a decrease of the fission cross sections for the even neutron number nuclides, being most evident in zone 4. For the same reason, capture cross sections increase toward EOL. In Table VIII, the corresponding fission probability $\sigma_f/(\sigma_c + \sigma_f)$ is shown. A high fission probability of americium results in a lower production rate of curium.

TABLE V

Actinide Inventory at the Beginning and at the End of the Fuel Cycle*

Isotope	0 Days	1400 Days	Δ_{tot} (%)
^{238}Pu	117	182	56
^{239}Pu	880	587	−33
^{240}Pu	706	649	−8.2
^{241}Pu	309	187	−40
^{242}Pu	318	312	−0.76
^{241}Am	934	625	−33
^{243}Am	472	344	−27
^{244}Cm	248	248	0.03
^{245}Cm	36.2	36.4	0.68
All actinides	4020	3250	−19

*Unit: kg.

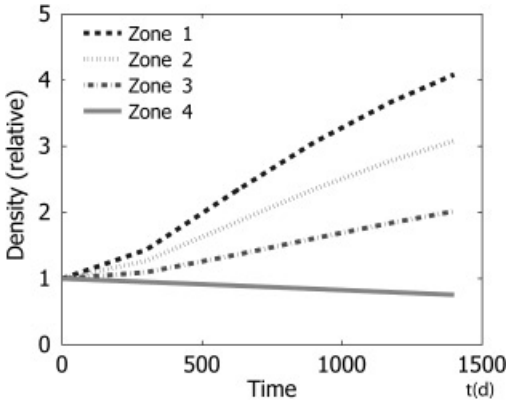

Fig. 6. ^{238}Pu density evolution in the different fuel zones of the core. The production of ^{238}Pu is largest in zone 1, having the largest americium concentration.

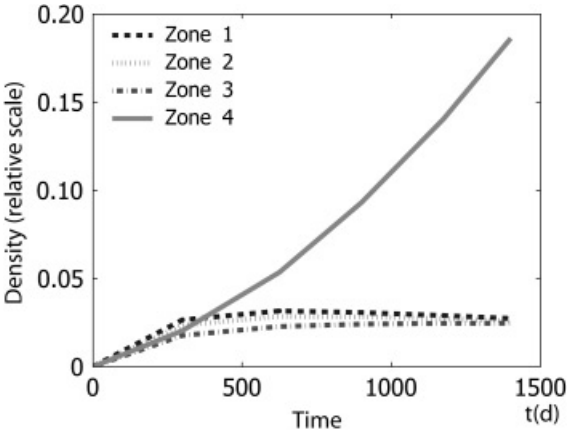

Fig. 7. ^{242}Cm density evolution. Note the effect of the spectrum softening in zone 4. In absolute numbers the core-averaged Cm production is negligible.

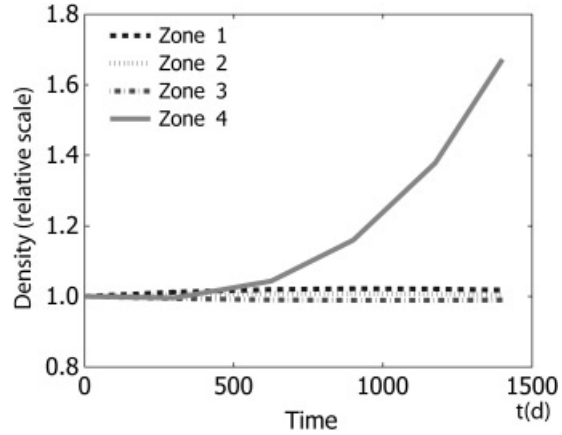

Fig. 8. ^{244}Cm density evolution. Note the effect of the spectrum softening in zone 4. In absolute numbers the core-averaged Cm production is negligible.

In order to compare the neutron spectrum in the present design with that resulting from use of liquid-metal coolants, we tabulate core-averaged cross sections for the sodium-cooled European fast reactor[35] (EFR) and the lead-bismuth–cooled accelerator transmutation of waste (ATW) design of Yang and Khalil[36] in Table IX. From the figures given in Table IX, one may expect that the use of helium coolant reduces the production of curium, as compared to transmutation of americium in sodium- or lead-bismuth–cooled systems. This is highlighted in Fig. 9, displaying the neutron spectrum in our core on top of that in the LBE-cooled ATW system.[36] The softer spectrum in the ATW design does have the advantage of increasing the burnup over fast fluence ratio. Accordingly, one may reach a higher burnup in the ATW design, reducing the number of reprocessing cycles.

TABLE VI

One-Group Cross Sections for Fission

	σ_f (b) Zone 1		σ_f (b) Zone 2		σ_f (b) Zone 3		σ_f (b) Zone 4	
Isotope	BOL	EOL	BOL	EOL	BOL	EOL	BOL	EOL
^{237}Np	0.56	0.48	0.59	0.35	0.61	0.24	0.66	0.15
^{238}Pu	1.32	1.25	1.34	1.13	1.36	1.02	1.41	0.96
^{239}Pu	1.67	1.66	1.67	1.66	1.68	1.71	1.68	1.89
^{240}Pu	0.61	0.52	0.63	0.40	0.66	0.29	0.71	0.21
^{241}Pu	1.92	1.98	1.90	2.10	1.89	2.32	1.88	2.85
^{242}Pu	0.47	0.39	0.49	0.29	0.52	0.19	0.55	0.12
^{241}Am	0.48	0.37	0.51	0.26	0.54	0.17	0.58	0.11
^{243}Am	0.39	0.29	0.41	0.20	0.43	0.13	0.47	0.07
^{244}Cm	0.78	0.62	0.75	0.46	0.78	0.32	0.83	0.22
^{245}Cm	2.07	2.10	2.06	2.21	2.06	2.43	2.05	3.01

TABLE VII

One-Group Cross Sections for Capture

	σ_c (b) Zone 1		σ_c (b) Zone 2		σ_c (b) Zone 3		σ_c (b) Zone 4	
Isotope	BOL	EOL	BOL	EOL	BOL	EOL	BOL	EOL
^{237}Np	0.79	0.89	0.76	1.07	0.74	1.36	0.70	1.97
^{238}Pu	0.27	0.30	0.26	0.37	0.26	0.47	0.24	0.69
^{239}Pu	0.23	0.25	0.22	0.31	0.21	0.42	0.20	0.64
^{240}Pu	0.28	0.31	0.27	0.37	0.26	0.48	0.25	0.67
^{241}Pu	0.38	0.41	0.38	0.44	0.37	0.50	0.36	0.64
^{242}Pu	0.23	0.26	0.23	0.32	0.22	0.41	0.21	0.58
^{241}Am	1.12	1.24	1.09	1.45	1.06	1.76	1.01	2.37
^{243}Am	0.90	1.01	0.87	1.20	0.85	1.50	0.81	2.17
^{244}Cm	0.32	0.35	0.31	0.41	0.30	0.50	0.29	0.76
^{245}Cm	0.16	0.18	0.16	0.22	0.15	0.28	0.15	0.41

TABLE VIII

Fission Probability $\sigma_f/(\sigma_f + \sigma_c)$

	Zone 1		Zone 2		Zone 3		Zone 4	
Isotope	BOL	EOL	BOL	EOL	BOL	EOL	BOL	EOL
^{237}Np	0.42	0.35	0.44	0.25	0.45	0.15	0.48	0.07
^{238}Pu	0.83	0.80	0.84	0.75	0.84	0.68	0.85	0.58
^{239}Pu	0.88	0.87	0.88	0.84	0.89	0.80	0.89	0.75
^{240}Pu	0.69	0.63	0.70	0.52	0.72	0.38	0.74	0.24
^{241}Pu	0.83	0.83	0.84	0.83	0.84	0.82	0.84	0.82
^{242}Pu	0.67	0.60	0.68	0.48	0.70	0.32	0.73	0.17
^{241}Am	0.30	0.23	0.32	0.15	0.34	0.09	0.37	0.04
^{243}Am	0.30	0.23	0.32	0.14	0.34	0.08	0.37	0.03
^{244}Cm	0.69	0.64	0.71	0.53	0.72	0.39	0.74	0.23
^{245}Cm	0.93	0.92	0.93	0.91	0.93	0.90	0.93	0.88

TABLE IX

Comparison of Cross Sections in Different Core Designs*

Isotope	This Design		ATW (Ref. 36)		EFR (Ref. 35)	
	σ_c	σ_f	σ_c	σ_f	σ_c	σ_f
^{237}Np	0.74	0.61	0.85	0.39	1.58	0.31
^{238}Pu	0.26	1.36	0.29	1.15	0.66	1.03
^{239}Pu	0.21	1.68	0.23	1.61	0.51	1.85
^{240}Pu	0.26	0.66	0.29	0.44	0.41	0.37
^{241}Pu	0.37	1.90	0.40	1.92	0.59	2.63
^{242}Pu	0.22	0.51	0.24	0.32	0.57	0.26
^{241}Am	1.06	0.53	1.23	0.30	1.84	0.28
^{243}Am	0.85	0.43	0.97	0.23	1.50	0.24
^{244}Cm	0.30	0.77	0.35	0.51	0.67	0.43
^{245}Cm	0.16	2.06	0.17	2.01	—	—

*At BOL in barns.

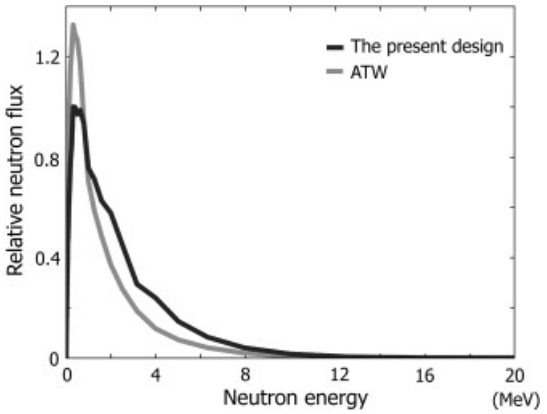

Fig. 9. Neutron flux spectrum in the present core. Comparison is made with the spectrum of the lead-bismuth–cooled core like in the ATW concept.[36] As expected, the spectrum of the gas-cooled core is harder.

VII. CONCLUSIONS

The excess of neutrons in a plutonium-fueled uranium-free fast reactor may be used to increase the P/D. By doing this it is possible to design a gas-cooled fast core with P/D = 1.8, providing sufficient cooling for decay heat removal during a postulated loss-of-pressure accident, while achieving efficient transmutation of minor actinides. At normal operation, a helium coolant pressure of 4.3 MPa is enough to keep cladding temperatures below 900 K, respecting limits of yield strength for irradiated cladding steels like 15-15Ti. The unusually small pressure drop of our core enables decay heat removal under natural circulation conditions with a heat exchanger elevation just more than 1 m above the core. The pumping power in the system under normal operation is as low as 5.9 MW, thanks to the low pressure drop. The calculated value of beta effective for this fuel type equals 140 pcm, which in conjunction with a vanishing Doppler feedback and a positive void worth of 6 $ makes subcritical operation mandatory. During 1400 days of full-power operation, 19.1% of the initial actinide mass is fissioned, and the most exposed fuel pin receives a dose of 170 dpa.

In summary, the present core design achieves the combined benefits of a hard spectrum and low pressure losses, allowing minimization of curium production while ensuring decay heat removal under a loss-of-flow or a postulated loss-of-pressure accident.

ACKNOWLEDGMENTS

The authors would like to thank W. Gudowski for providing Doppler-broadened cross-section files and M. Schikorr for clarifying discussions. This work was financially supported by SKB.

REFERENCES

1. EUROPEAN TECHNICAL WORKING GROUP ON ADS, "A European Roadmap for Developing Accelerator Driven Systems (ADS) for Nuclear Waste Incineration," ISBN 88-8286-008-6, ENEA (2001).

2. J. P. GROUILLER, S. PILLON, C. DE SAINT JEAN, F. VARAINE, L. LEYVAL, G. VAMBENEPE, and B. CARLIER, "Minor Actinides Transmutation Scenario Studies with PWRs, FRs and Moderated Targets," *J. Nucl. Mater.*, **320**, 163 (2003).

3. A. VASILE, P. DUFOUR, H. GOLFIER, J. P. GROUILLER, J. L. GUILLET, C. POINOT, G. YOUINOU, and A. ZAETTA, "Advanced Fuels for Plutonium Management in Pressurized Water Reactors," *J. Nucl. Mater.*, **319**, 173 (2003).

4. J. WALLENIUS and M. ERIKSSON, "Neutronics of Minor-Actinide Burning Accelerator-Driven Systems with Ceramic Fuel," *Nucl. Technol.*, **152**, 367 (2005).

5. "Review of PNL Study on Transmutation Processing of High Level Waste," D. G. FOSTER, Ed., LA-UR-74-74, Los Alamos National Laboratory (1974).

6. T. TAKIZUKA, H. TAKADA, I. KANNO, T. NISHIDA, M. AKABORI, and Y. KANEKO, "Conceptual Design of Transmutation Plant," *Proc. Specialist Mtg. Accelerator-Driven Transmutation Technology for Radwaste and Other Applications*, Stockholm, Sweden, June 24–28, 1991.

7. K. TSUJIMOTO, T. SASA, K. NISHIHARA, H. OIGAWA, and H. TAKANO, "Neutronics Design for Lead-Bismuth Cooled Accelerator-Driven System for Transmutation of Minor Actinide," *J. Nucl. Sci. Technol.*, **41**, *1*, 21 (2004).

8. B. CARLUEC and P. ANZIEU, "Proposal for a Gas Cooled ADS Demonstrator," *Proc. 3rd Int. Conf. Accelerator Driven Transmutation Technologies and Applications (ADTTA'99)*, Praha, Czech Republic, June 7–11, 1999.

9. G. B. MELESE-D'HOSPITAL, "Review of Gas Cooled Reactors Thermal Hydraulics," *Proc. ANS/ASME/NRC Int. Topl. Mtg. Nuclear Reactor Thermal-Hydraulics*, Saratoga Springs, New York, October 5–8, 1980.

10. J. P. GAILLARD, G. MIGNOT, and A. CONTI, "Thermal-Hydraulic Design of a Gas Cooled Fast Reactor," *Proc. 2003 Int. Congress Advances in Nuclear Power Plants (ICAP '03)*, Córdoba, Spain, May 4–7, 2003, American Nuclear Society (2003) (CD-ROM).

11. E. E. FELDMAN and T. Y. C. WEI, "Cold-Finger Concept for Passive Decay Heat Removal in Gas-Cooled Reactors," *Trans. Am. Nucl. Soc.*, **88**, 681 (2003).

12. P. FORTESCUE, G. B. MELESE-D'HOSPITAL, J. PEAK, and L. MEYER, "A Developmental Gas-Cooled Fast Breeder Reactor Plant," *Proc. Nuclex 69*, Basel, Switzerland, October 6–11, 1969.

13. J. B. DEE and G. B. MELESE-D'HOSPITAL, "Part 1—The 300 MW(e) GCFR Demonstration Plant," *Mech. Eng.*, **94**, 18 (1972).

14. M. ERIKSSON, J. WALLENIUS, M. JOLKKONEN, and J. E. CAHALAN, "Inherent Safety of Fuels for Accelerator-Driven Systems," *Nucl. Technol.*, **151**, 314 (2005).

15. N. CHAUVIN, J. C. GARNIER, J. L. SERAN, P. MARTIN, and P. BROSSARD, "Requirements for Fuel and Structural Materials for Gas Cooled Fast Reactor (GFR), Preliminary Design," *Proc. Global 2003*, New Orleans, Louisiana, November 16–20, 2003, American Nuclear Society (2003) (CD-ROM).

16. J. WALLENIUS, "Neutronic Aspects of Inert Matrix Fuels for Application in ADS," *J. Nucl. Mater.*, **320**, 142 (2003).

17. J. WALLENIUS, K. MINATO, and Y. ARAI, "Influence of ^{15}N Enrichment on Neutronics, Costs and ^{14}C Production in Nitride Fuel Cycle Scenarios," *J. Nucl. Mater.* (submitted for publication).

18. R. THETFORD and M. MIGANELLI, "The Chemistry and Physics of Modelling Nitride Fuels for Transmutation," *J. Nucl. Mater.*, **320**, 44 (2003).

19. L. ZABOUDKO, "Status of CEA-Minatom Collaborative Experiment Bora-Bora: Fuels with High Plutonium Content," *Proc. ANL Transmuter Fuel Development Workshop*, Idaho Falls, Idaho, November 19–21, 2001.

20. J. CETNAR, J. WALLENIUS, and W. GUDOWSKI, "MCB: A Continuous Energy Monte-Carlo Burnup Simulation Code, Actinide and Fission Product Partitioning and Transmutation," *Proc. 5th Int. Information Exchange Mtg.*, Mol, Belgium, November 25–27, 1998, p. 523, Organization for Economic Cooperation and Development/Nuclear Energy Agency (1998).

21. "NEA-1643 MCBIC," available on the Internet at ⟨http://www.nea.fr/abs/html/nea-1643.html⟩ (Feb. 15, 2005).

22. "Actinide and Fission Product Partitioning and Transmutation—Status and Assessment Report," Organization for Economic Cooperation and Development/Nuclear Energy Agency (1999).

23. M. DALLE DONNE and L. MEYER, "Turbulent Convective Heat Transfer from Rough Surfaces with Two-Dimensional Rectangular Ribs," *Int. J. Heat Mass Transfer*, **20**, 583 (1977).

24. M. KAVIANY, *Principles of Heat Transfer in Porous Media*, Springer-Verlag, New York (1999).

25. *CRC Handbook of Chemistry and Physics*, 73rd ed., D. R. LIDE, Ed., CRC Press, Boca Raton, Florida (1992).

26. N. SCOTT CANNON, F. H. HUANG, and M. L. HAMILTON, "Transient and Static Mechanical Properties of D9 Fuel Pin Cladding and Duct Material Irradiated to High Fluence," *Proc. 15th ASTM Int. Symp. Effects of Radiation on Materials*, Nashville, Tennessee, 1992, ASTM STP 1125, American Society for Testing and Materials (1992).

27. R. J. PUIGH and M. L. HAMILTON, "In-Reactor Creep Rupture Behavior of the D19 and 316 Alloys," *Proc. Influence of Radiation on Material Properties: 13th Int. Symp. (Part II)*, Seattle, Washington, June 23–25, 1986, American Society for Testing and Materials (1987).

28. J. L. SÉRAN et al., "Behaviour Under Neutron Irradiation of the 15-15 Ti and Em10 Steels Used as Standard Materials of the PHÉNIX Fuel Subassembly," *Proc. 15th ASTM Int. Symp. Effects of Radiation on Materials*, Nashville, Tennessee, 1992, ASTM STP 1125, American Society for Testing and Materials (1992).

29. GROUPE DE TRAVAIL RAMSES 2, "Règles d'analyse mécaniques des stuctures irradiées," CEA R.5618, Commissariat à l'Energie Atomique.

30. G. B. MELESE-D'HOSPITAL, "Natural Circulation Cooling Potential of CO2 and He for GCFR's," *Proc. ANS/ASME/NRC Int. Topl. Mtg. Nuclear Reactor Thermal-Hydraulics*, Saratoga Springs, New York, October 5–8, 1980.

31. N. E. TODREAS and M. S. KAZIMI, *Nuclear Systems I—Thermal Hydraulic Fundamentals*, Hemisphere Publishing Company, New York (1989).

32. A. E. WALTAR and A. B. REYNOLDS, *Fast Breeder Reactors*, Pergamon Press, New York (1981).

33. M. A. HASSAN and K. REHME, "Heat Transfer near Spacer Grids in Gas-Cooled Rod Bundles," *Nucl. Technol.*, **52**, 401 (1981).

34. *The Nuclear Fuel of Pressurized Water Reactors and Fast Reactors—Design and Behavior*, H. BAILLY, D. MÉNESSIER, and C. PRUNIER, Eds., Commissariat à l'Energie Atomique (1999).

35. H. W. WIESE, "Actinide Transmutation Properties of Thermal and Fast Fission Reactors Including Multiple Recycling," *J. Alloys Compounds*, **271**, 522 (1998).

36. W. S. YANG and H. S. KHALIL, "Blanket Design Studies of a Lead-Bismuth Eutectic–Cooled Accelerator Transmutation of Waste System," *Nucl. Technol.*, **135**, 162 (2001).

37. C. W. HUNTER, R. L. FISH, and J. J. HOLMES, "Mechanical Properties of Unirradiated Fast Reactor Cladding During Simulated Overpower Transients," *Nucl. Technol.*, **27**, 376 (1975).